The Geomagnetic Storm-Time Response to Different Solar Wind Driving Conditions

C. Robert Clauer

University of Michigan, Center for Space Environment Modeling, Ann Arbor, MI 48109-2143

Abstract. Geomagnetic storms are phenomena that have the potential for serious space weather impact on a variety of technologies deployed in space and on the ground. Geomagnetic storms can result from a variety of solar wind driving conditions and storms can vary considerably in their severity. Geomagnetic storms also exhibit a variety of internal magnetospheric convection modes, including storm time substorms, periods of enhanced steady magnetospheric convection and periods of global sawtooth oscillations. The paper reviews our present understanding of the geomagnetic storm response to different driving conditions in the solar wind and the different magnetospheric convection modes that can develop during storm time conditions. Our understanding, based upon statistical and case example investigations, is reviewed along with open questions in our understanding.

Index Terms. Geomagnetic Storms, solar wind-magnetosphere coupling, magnetospheric convection

1. Introduction

Dungey, (1961) introduced the concept that magnetic reconnection is the driver of magnetospheric convection. According to the Dungey concept, convection begins when the interplanetary magnetic field carried by the solar wind merges with the geomagnetic field at an x-line located at the sub-solar point on the dayside magnetopause. The solar wind carries the interconnected field lines over the polar caps creating a long magnetic tail. The interconnected (or open) field lines reconnect at a nightside x-line and then the newly closed field lines move sunward around the Earth to return to the dayside. Due to the electrical linkage between the magnetosphere and ionosphere, this process also creates a 2-cell convection pattern in the ionosphere. The equivalent current system associated with this 2-cell pattern has been termed the DP2 (disturbance polar type 2) current pattern.

The growth phase model of the substorm developed with the recognition that the dayside reconnection rate could increase substantially without a simultaneous increase in the nightside rate. This is possible because of the large dimensions of the magnetospheric system and the time required to propagate information from the dayside x-line to the nightside x-line. The mismatch of reconnection rates results in a period of energy loading in the tail lobes as the dayside magnetopause is eroded and flux is transported tailward faster than the flux return from the nightside x-line. In addition, pressure gradients in the inner magnetosphere will cause plasma from the inner plasma sheet to flow sunward, thus causing the near-Earth plasma sheet to thin. The thin plasma sheet eventually becomes unstable and a new near Earth x-line forms thus initiating the substorm expansion phase. Lobe flux is eventually reconnected at the new near-Earth x-line and returns to the dayside more rapidly than the reconnection at the distant x-line. This sequence of events has formed the 'loading – unloading' paradigm for substorms in which the initial period of flux transport and energy accumulation in the tail lobe is called the loading or growth phase portion of the substorm and the new neutral line formation and rapid conversion of stored magnetic energy to particle kinetic energy has been called the substorm expansion phase.

A view that was dominant for many years was that, with the exception of quiet conditions, steady state input-output flow was not possible. For example, Kamide et al.,(1977) showed that substorms occur with 100% probability whenever the northward component of the 1-hour averaged IMF is -3 nT or less. Borovsky et al., (1993) determined through a large statistical investigation that the substorm recurrence period, on average, is about 2.7 hours. Theoretical considerations also suggest that substorms are the primary element of magnetospheric dynamics. Simple analogue models that describe the magnetosphere using currents, generators and loads produce an inherent periodic response to steady enhanced external driving (Baker et al., 1990; Klimas et al.,1992). MHD calculations in the tail plasma sheet also indicate that steady earthward convection leads to an unstable region ('pressure catastrophy') in the inner magnetospheric configuration where the magnetic field strength increases due to the increasing dipole contribution (Erickson, 1992).

The original Dungey model, on the other hand, depicted a balanced convection system and this idea was revisited when Pytte et al., (1978) identified periods of enhanced magnetic activity that also were characterized by a 2-cell (DP2-like) ionospheric convection with no evidence for substorm expansions. These disturbances were named convection bays for the extended period of enhanced auroral AL activity and it was speculated that these periods were a manifestation of enhanced but balanced dayside and nightside reconnection. Sergeev, (1977) studied similar events and established that enhanced solar wind energy input to the magnetosphere may either lead to substorms or enhanced, but steady convection. The term convection bay has now been replaced by 'Steady Magnetospheric Convection' (SMC) events and a thorough review of SMC research has been published by Sergeev et al., (1996). Many of the convection bays investigated by

Pytte et al., (1978) were during periods of strong disturbance with the implication that dayside and nightside convection rates can balance during very strong driving. Sergeev et al., (1996), however, suggests that balanced convection can develop only during moderate activity and that strong activity will include imbedded substorms.

Recently, there has been considerable advancement in our understanding of geomagnetic storms due to improved global data visualization and advances in both theory and modeling. This has led to a new paradigm, expressed at the Chapman Conference in Lonavala, in our understanding of ring current development – the defining characteristic of geomagnetic storms (Sharma et al., 2003).

The conventional paradigm, that has been held for the past 20 years or longer, was based on the view that the storm main phase rapidly produced a symmetric ring current that provided the most important component of the D_{st} index. The geomagnetic storm was thought to result from an accumulation of many elementary disturbances called substorms (Akasofu and Chapman, 1961; Chapman, 1962). Each successive substorm produces an enhanced westward electric field near the outer ring current boundary. This enhanced induction electric field brings particles in from the plasma sheet – a process called the substorm injection. The injected particles become trapped on closed azimuthal drift paths. Since the trapped ions and electrons drift in opposite directions due to their gradient and curvature drifts, a westward azimuthal ring current is produced.

The new paradigm that was adopted at Lonavala (the Lonavala consensus) asserts that ring current development results from a sustained enhancement of the convection electric field (Clauer and McPherron, 1980; Kamide, 1992; McPherron, 1997; Liemohn et al., 1999, 2001b, a; Liemohn, 2003; Clauer et al., 2003, and references therein). In this view, most of the ring current magnetic perturbations during the storm main phase are due to a partial ring current which closes, in part, through the ionosphere, and in part, through the magnetopause. The effect of the enhanced cross-magnetospheric electric field is to move the Alfven layers inward with the consequence of further energizing plasma and also moving the current closer to the Earth. Only after the enhanced convection electric field is reduced do particles find themselves on closed azimuthal drift paths and the ring current becomes symmetric. This occurs during the recovery phase. The 2-phase decay of D_{st} is explained in the new paradigm with the rapid initial decay due to plasma on open drift paths convecting out of the system and the slow decay due to charge exchange within the trapped population.

The view that substorms are the elementary units of magnetospheric dynamics has produced a research focus on isolated substorms whereas periods of continuous activity have received less attention (Fairfield, 1992). Periods of more intense activity, however, are receiving much more attention now, in part, becuase of the interest in understanding, modeling, and forecasting space weather. While considerable investigation has been devoted to the study of magnetic storms, many of these studies have focused on modeling the development of the D_{st} index as a proxy for the energy content of the symmetric ring current. The ability of models to provide detailed output that considers the temporal and spatial development of storms enables the direct comparison with data to validate model results (e.g. Liemohn, 2003, Clauer et al., 2003) and is improving our physical understanding of magnetic storms.

2.Storms during high speed streams

During the declining phase of the solar cycle, geomagnetic activity and storms are often associated with high speed streams that emerge from coronal holes. Figure 1 shows ACE measurements of the solar wind and IMF during March 15, 2003 when the solar wind velocity was between 600 km/s and 650 km/s. Also shown are, from the top, the IMF Bx, By, and Bz components, solar wind number density and velocity. Note that the IMF Bz component shows frequent short-duration southward fluctuations. This implies that there are frequent short periods of magnetospheric loading.

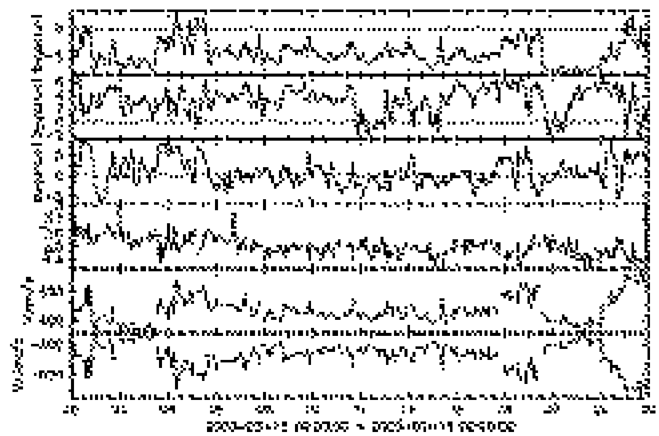

Fig. 1. ACE satellite measurements of the solar wind and Interplanetary Magnetic Field in GSM coordinates at the L1 position upstream from the Earth.

The geomagnetic activity produced by the high speed stream driving on March 15, 2003 is shown in Figure 2. The bottom panel shows the provisional auroral indices for March 15, 2003 and the top panel shows a map of the world-wide low latitude magnetic disturbance field. The contour map shows the low latitude disturbance field (quiet field removed) as a function of local time and universal time. Positive perturbations are shown with contours that have blue shading and negative perturbations are shown with contours that have red shading. The AL index shows a series of intensifications that are also associated with low-latitude positive magnetic bays observed on the night side and indicated with vertical lines. These are a series of periodic substorm expansions. The result of this activity is a small geomagnetic storm in which the SYM-H index reaches -56 nT.

Next, we examine measurements of the energetic particle fluxes measured at geostationary orbit that are thought to be directly associated with the development of the storm time ring current. In Figure 3 we show the energetic proton flux measured by the Los Alamos National Laboratory geostationary satellites on March 15, 2003. Each panel shows the energetic proton fluxes measured at a different geostationary satellite. The blue triangle mark local midnight at each satellite. The red triangle marks local noon at each satellite. Each of the substorm expansions shows the 'injection' signature of energetic particles at the geostationary satellites near local midnight. The 'injection' signature consists of a simultaneous enhancement of the energetic particle fluxes in all energy channels (no energy dispersion) to values above the initial quiescent value. We note here that the injections are localized on the night side and that energy dispersion is observed at satellites away from the injection region with higher energies (bottom curves) arriving earliest.

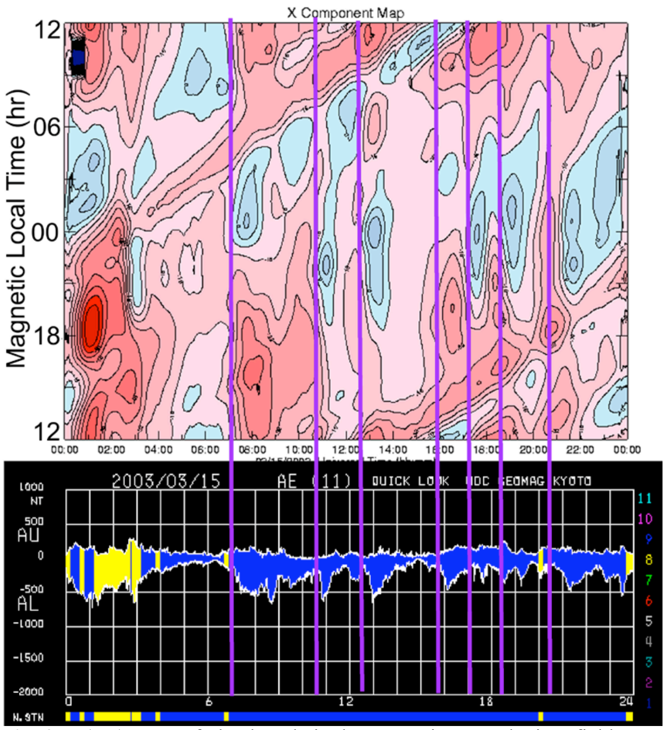

Fig. 2. (top) Map of the low latitude magnetic perturbation field as a function of local time (vertical axis) with midnight in the center and local noon at the edges, and Universal time (horizontal axis) during March 15, 2003. Contours are at 5nT intervals. Red shading indicates field decrease and blue shading indicated a field increase. (bottom) Provisional AU and AL indices. The color scale indicates the number of stations used to compute the indices. Vertical lines show each substorm expansion phase onset.

3. Storms during Magnetic Clouds

Coronal Mass Ejections (CMEs) generally form a large magnetic flux rope that propagates into interplanetary space. The large flux rope contains very low density and a strong field that is observed to slowly rotate as the rope passes an observer. The ICME flux rope is often referred to as a magnetic cloud and if the cloud is oriented properly, it will produce a long steady period of slowly varying southward IMF at the magnetopause. If the flux rope is propagating faster than the Alfven velocity through the ambient solar wind plasma, a shock front and sheath will form in front of the cloud. The sheath may also contain a large southward IMF for a substantial period prior to the encounter with the magnetic cloud. Some of the most severe magnetic storms, the so-called 'double hit storms' develop in response to these two subsequent intervals of sustained strong southward IMF at the magnetopause.

As noted in the introduction, periods of steady sustained southward IMF, such as can exist in an ICME flux rope, can lead to enhanced Steady Magnetospheric Convection. Figure 4 shows the solar wind and IMF during February 3, 1998 where the vertical lines mark an interval with relatively steady southward IMF. Examination of the geomagnetic activity that resulted from the interaction of this sola wind and IMF with the magnetosphere exhibits SMC characteristics.

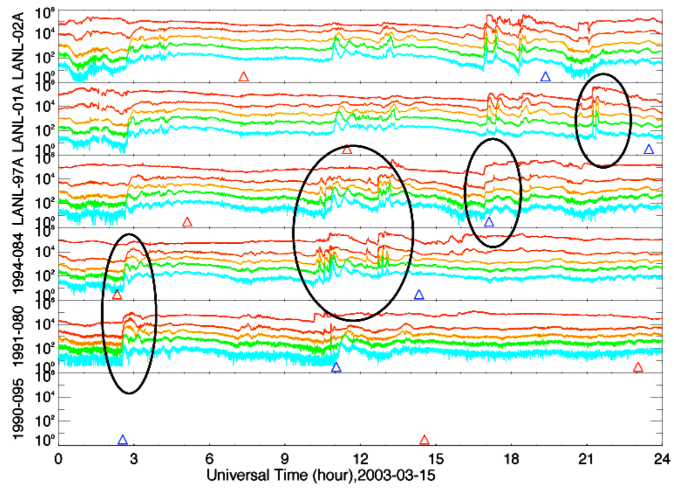

Fig. 3. Energetic proton fluxes measured at geostationary orbit by LANL satellites during March 15, 2003. Red triangles indicate local noon and blue trianglesindicate local midnight at each satellite. Substorm injection signatures localized in local time are indicated.

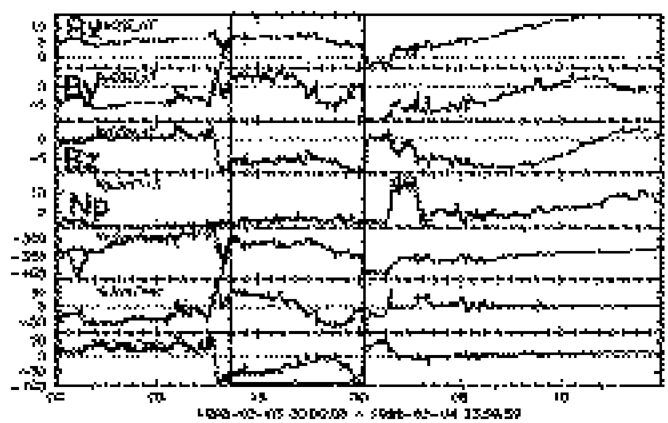

Fig. 4. ACE measurements of IMF and solar wind on Feb 3, 1998. The vertical lines mark a period of quasi-steady southward IMF.

During SMC periods, the dayside and nightside reconnection rates must balance and therefore there should be no additional increase in tail lobe magnetic flux. Since the lobe magnetic field maps to the high latitude polar cap, we utilize the area of the polar cap determined from global auroral images to identify periods when the area remains nearly constant. Increasing polar cap area would imply the loading of energy into the tail lobes while decreasing polar cap area would imply a reduction of energy in the lobe magnetic field (DeJong and Clauer, 2005).

In Figure 5 we provide an analysis of polar cap dynamics during the Feb 03, 1998 event. Figure 5 shows a summary plot of parameters determined from Polar global auroral images for Feb 03, 1998. The top panel shows a summary of the auroral images obtained during the day. The vertical axis is magnetic local time, and we plot the brightest pixel measured at each local time for each image. This permits us to identify auroral intensifications during the study interval. The other panels are the total particle energy flux estimated from the global auroral emissions, the polar cap area, the polar cap electric potential drop, Dst index, AE index and IMF Bz component. In this example we find the auroral particle energy flux, polar cap area, and polar cap potential drop are nearly constant during the interval 15 UT – 24 UT.

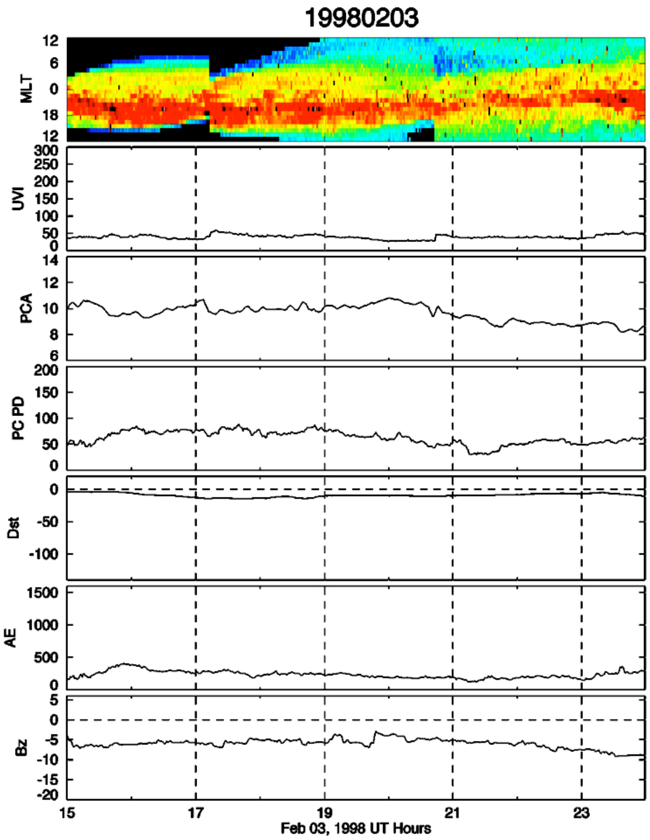

Fig. 5. Stack plot of data from Polar UVI and magnetic indices from the SMC event on February 3, 1998. From the top (a) MLT-UT map of the maximum photon flux, (b) auroral energy flux, (c) Polar cap area, (d) cross polar cap potential difference, (e) Dst, (f) Ae, (g) IMF Bz

Figure 6 shows the low latitude disturbance field and auroral electrojet indices in the same format as Figure2. The westward auroral electrojet show an overall enhancement without the punctuation of substorm expansion onsets and there is no indication of substorm expansions in the low latitude magnetic disturbance. Figure 7 shows the lack of injection signatures in the geostationary LANL satellite energetic proton data during the SMC event. February 3, 1998 is at best a minor storm, but it illustrates our identification of SMC intervals well.

It has been recently recognized that strong steady driving can lead to a phenomena called global sawtooth oscillations. Sawtooth oscillations are quasi-periodic, large-amplitude oscillations observed globally in the energetic particle differential flux measurements at geostationary orbit. They derive the name sawtooth oscillations because of the shape – a series of slow flux decreases followed by rapid increases – that resemble the teeth of a saw blade. The sawtooth-like flux variations are indicative of changes in the morphology of the magnetic field in the inner magnetosphere undergoing strong stretching and then rapid dipolarization. The period of oscillation is between 2 - 4 hours and the dipolarization phase lasts between 5 and 15 minutes. The remarkable and unique aspect of sawtooth oscillations is that they are observed over a very broad range of local times, including sometimes, well into the dayside magnetosphere.

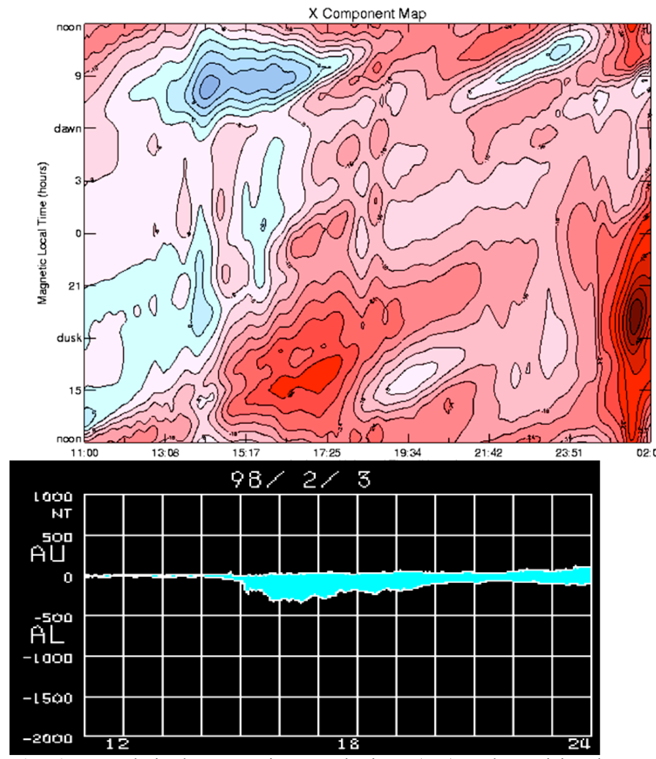

Fig. 6. Low latitude magnetic perturbations (top) and provisional auroral indices (bottom) on Feb 3, 1998 in same format as Fig. 2.

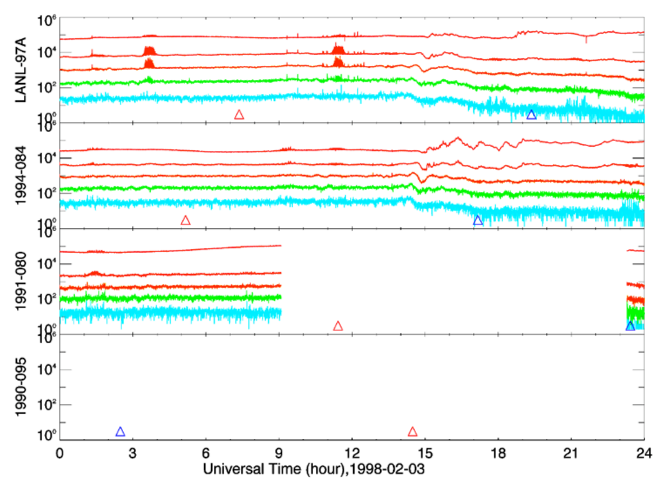

Fig. 7. Energetic proton fluxes at geostationary orbit during SMC event on Feb 3, 1998 measured by LANL satellites in the same format as Fig.3.

LANL energetic proton data for the November 13, 1998 magnetic storm that contained several sawtooth oscillations is shown in Figure 8. Also shown at the bottom of the plot is the magnetic field inclination angle in GSM coordinates measured at the GOES-8 satellite located near magnetic midnight. (0º is parallel to the X-Y plane and 90º is orthogonal to the X-Y plane. The GOES data shows a series of slow, stretching of the field followed by a rapid depolarization. The angular changes (40º - 60º) in the field tilt are extremely large compared with typical substorm dipolarizations (15º - 30º) (Borovsky et al., 2006).

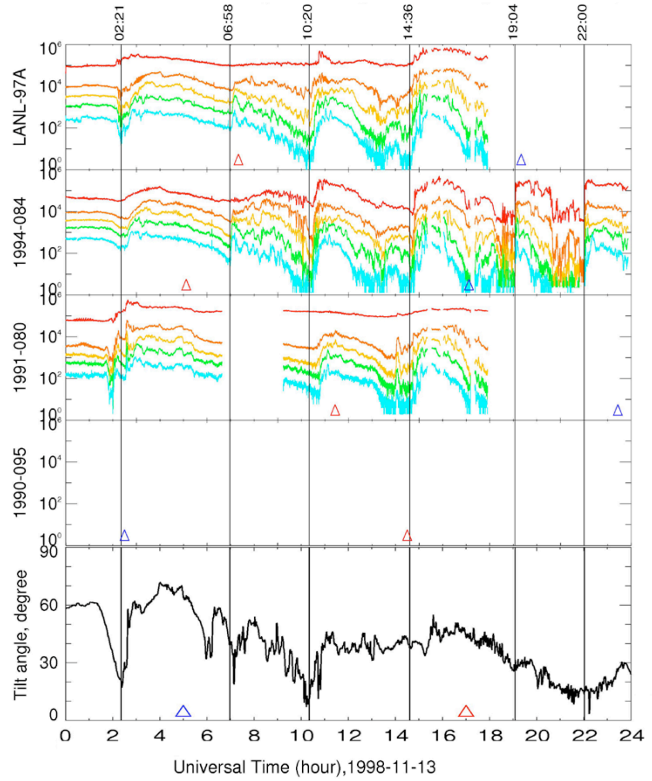

Fig. 8. LANL geostationary satellite measurements of energetic proton fluxs during global sawtooth injections (top) and GOES magnetic field inclination angle (bottom). Vertical lines mark sawtooth injections.

Vertical lines in Figure 8 are drawn for each sawtooth injection and depolarization. The line is drawn at the time of the earliest signature. (Henderson et al., 2006) shows that the dispersionless component of the injection during sawtooth events is confined to the nightside and evening side of the magnetosphere, but is much broader in local time extent than typical substorm injections. While the injection signatures are seen globally, there is generally a small energy dispersion and drift delay in the observations near mid-day.

As noted above, sawtooth events are often observed during strong steady driving conditions. Figure 9 shows the upstream solar wind conditions during November 13, 1998 storm which contained a series of sawtooth oscillations. The ACE satellite measured the IMF Bz component to be around –15nT from about 5 UT through the rest of the day to provide constant and steady magnetospheric driving. A series of sawtooth oscillations with a period of about 4 hours begins around 6 UT.

The ground magnetic observations during the November 13 1998 storm and sawtooth event are displayed in Figure 10. Vertical lines are drawn at the injection times taken from Figure 8. Typical substorm magnetic signatures are observed, positive bays at low latitudes (nested contours of increasing field perturbation), and enhancement in the westward electrojet reflected in the Al index. The storm development is seen predominantly in the development of a large partial ring current that depresses the field (red shaded contours) on the afternoon and evening side of the Earth.

Global sawtooth oscillations occur during some but not all geomagnetic storms. September 24-25, 1998 is another magnetic storm that has undergone considerable community investigation. This storm contains periods of both strong SMC as well as sawtooth oscillations. It is a storm that results from an ICME shock followed by a geoeffective magnetic cloud. The shock and cloud portion of the ICME are indicated on Figure 11. The initial shock is observed upstream at WIND at 23:10 UT and the SSC is observed in ground magnetograms at 23:40.UT. During the cloud, the IMF Bz component is relatively steady with values between –10 and –20 nT.

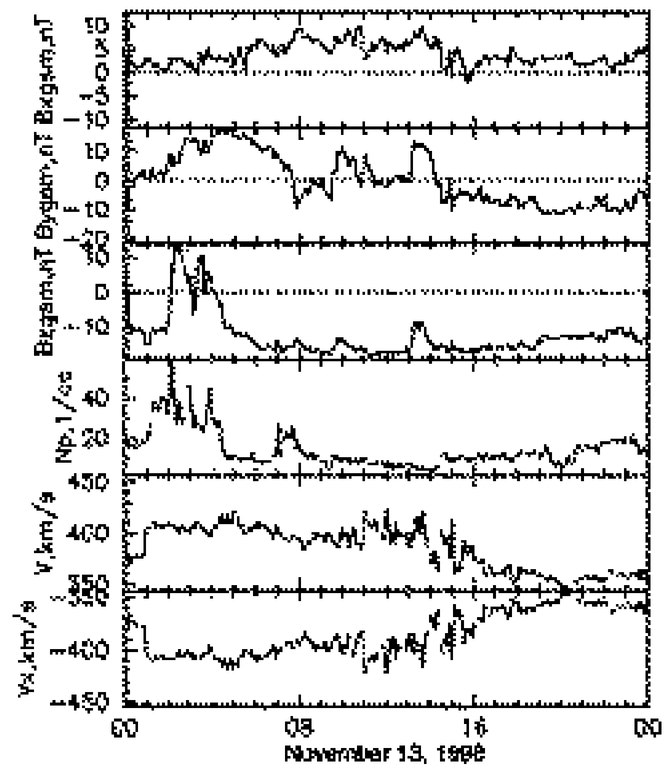

Fig. 9. ACE satellite measurements of IMF and solar wind on November 13, 1998.

Following the SSC at about 23:40 UT on September 24, 1998, a storm main phase was initiated at about 01:50 UT on September 25 in response to the strongly southward IMF apparent in the ICME shock sheath at the magnetopause. From 01:50 UT to 06 UT, a strong partial ring current develops with maximum perturbation centered near 21 MLT. There are no substorm signatures until 06:10 UT and this is followed by a series of sawtooth oscillations with period of about 2 hours. Vertical lines in Figure 12 mark the sawtooth injections and associated enhancements (positive bay signatures) measured in the low latitude ground magnetic perturbations. This is a rather complex event because there are several large changes in the solar wind dynamic pressure during the storm, so the identification of features presented here should be considered somewhat tentative.

In summary, this data presentation show a variety of storm time activity that results from different solar wind driving conditions. This activity includes a series of periodic classical substorms where the driver is a high-speed stream and the Bz component of the IMF contains frequent short duration southward fluctuations. This produces a minor storm interval measured by the Dst index. During CME related magnetic cloud events, we find generally larger storms. These storm time periods can contains periods of steady magnetospheric convection, substorm expansions and periodic sawtooth oscillations. We show an example of steady magnetospheric convection during an interval of weak but steady driving and also during a period of strong but steady driving.

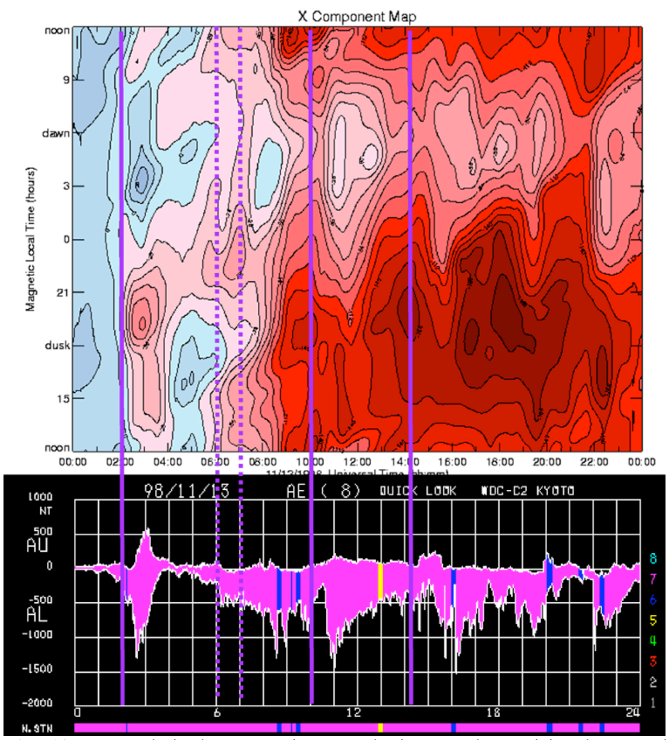

Fig. 10. Low latitude magnetic perturbations and provisional auroral indices on Nov 13, 1998 in same format as Fig. 2. Vertical lines mark substorm expansion or sawtooth onsets.

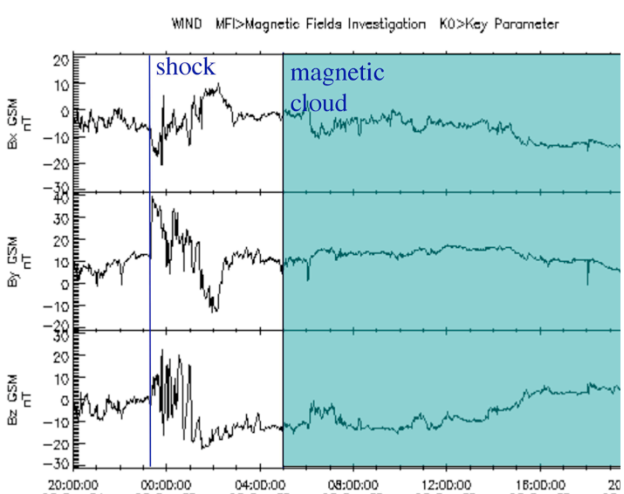

Fig. 11. WIND upstream IMF measurements on Sept 24 – 25, 1998 of ICME shock and magnetic cloud.

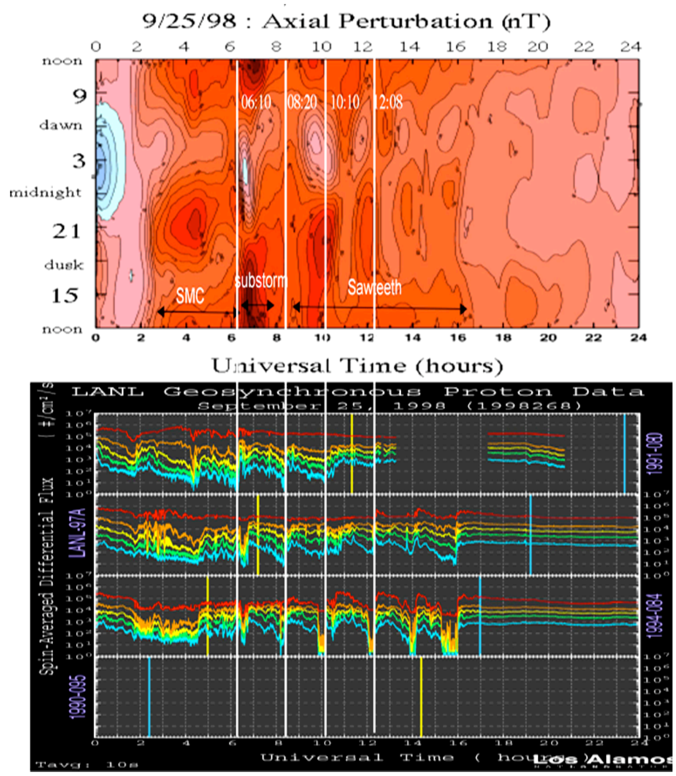

Fig. 12. Low latitude magnetic perturbation LT-UT map and LANL geostationary satellite energetic proton data for the Sept 25, 2998 storm interval.

4. Discussion

(Borovsky et al., 2006) shows the results of a statistical investigation of the solar wind driving conditions during different magnetic activity divided according to periodic classic substorms (similar to the example shown here), sawtooth periods, and SMC periods.

Figure 13 shows the statistical distribution of the solar wind driving measured as –VBz for SMC intervals, sawteeth intervals, and intervals of periodic substorms identified during the period 1963 – 2004. The sawtooth distribution is clearly different and suggests that they develop during periods of stronger driving.

Figure 14 show the distributions as a function of solar wind turbulence measured by $\delta B/B$. It shows that periodic substorms result during periods of greater turbulance while SMC and sawtooth events develop during quasi-steady driving.

Figure 15 shows the distributions of solar wind magnetosonic Mach number measured during periods of sawtooth events, periodic substorm intervals and SMC intervals. The sawtooth intervals are clearly unique with low mach number, consistent with the low density in the magnetic cloud. Figure 16 also shows that sawtooth intervals are unique in that the magnetosheath β value is unusually small.

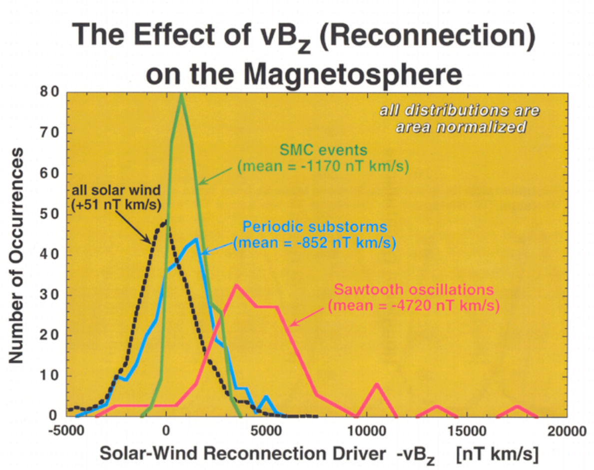

Fig. 13. Values of –vBz of the solar wind, integrated over time form one substorm onset to the next, one sawtooth depolarization onset to the next, and during SMC intervals, respectively for periodic substorms, sawtooth events and SMC intervals after Borovsky et al., 2006.

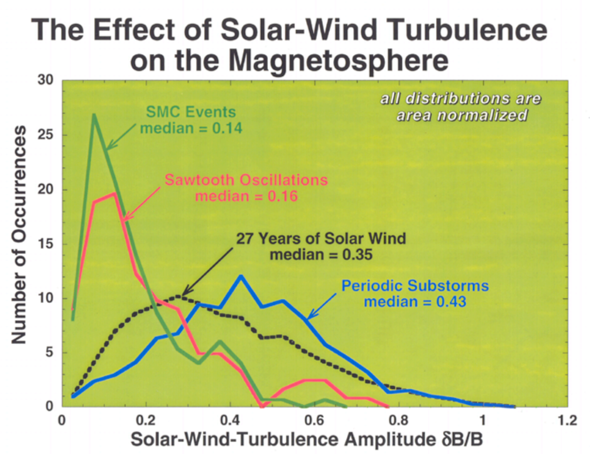

Fig. 14. Distributions of the values of δB/B during SMC intervals, periodic substorm intervals and sawtooth event intervals after Borovsky et al., 2006.

The low-β magnetosheath will have some unique properties that include relatively stiff magnetic field lines and low levels of MHD fluctuations. This will also lead to an asymmetric shape of the bow shock and flow pattern around the magnetosphere depending on the orientation of the magnetic field. The low mach number solar wind suggests that the compression across the bow shock will be weak and the width of the magnetosheath will be greater than normal.

Advancment in our understanding should take into account the differences in magnetospheric response to the different driving conditions identified in the above examples and in the statistical results from (Borovsky et al., 2006). There is speculation that reconnection during low mach number conditions may be more efficient and therefore produce larger cross magnetospheric electric fields in the inner magnetosphere.

Another area for investigation should focus on the differences in tail reconnection that may develop during classic substorm expansions and during sawtooth dipolarizations. While the classic substorm expansion involves the reconnection of considerable lobe flux to release the stored magnetic energy, there is speculation that sawtooth events involve primarily the reconnection of closed flux in the plasma sheet with little additional lobe flux reconnection. Another major problem to resolve is to determine the external and internal conditions that lead to either SMC or Sawtooth intervals, since both seem to occur during periods of steady solar wind driving.

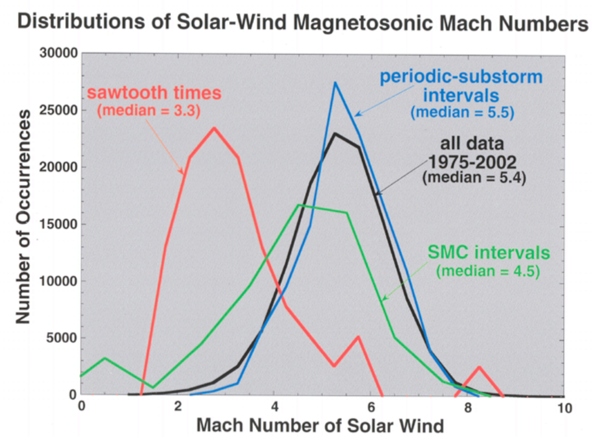

Fig. 15. Distributions of solar wind magnetosonic mach number during sawtooth intervals, periodic substorm intervals and SMC intervals after Borovsky et al., 2006.

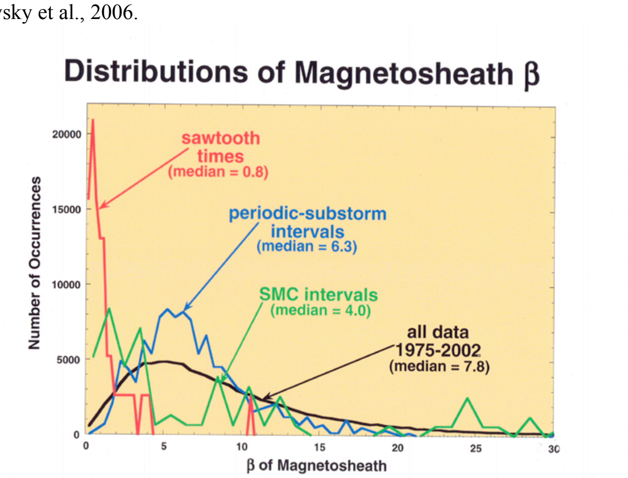

Fig. 16. Distributions of magnetosheath plasma β during sawtooth intervals, periodic substorm intervals and SMC intervals after Borovsky et al., 2006.

Acknowledgments. This work has been supported by NASA grants NAG5-12176 and NAG5-12040 and by the National Science Foundation grants OPP-0220735 and ATM-0325332. I am grateful to Joe Borovsky, Mike Henderson, Anna DeJong, Xia Cai and Dan Welling who have contributed substantially to many of the results presented here.

References

Akasofu, S.-I., and S. Chapman, The ring current, geomagnetic disturbance and the Van Allen radiation belts, *J. Geophys. Res.*, *66*, 1321, 1961.

Baker, D. N., A. J. Klimas, R. L.McPherron, and J. B¨uchner, The evolution from weak to strong geomagnetic activity: An interpretation in terms of deterministic chaos, *Geophys. Res. Lett.*, *17*, 41, 1990.

Borovsky, J., R. J. Nemzek, and R. D. Belian, The occurrence rate of magnetopheric-substorm onsets: Random and periodic substorms, *J. Geophys. Res.*, *98*, 3807–3813, 1993.

Borovsky, Joseph E., Robert J.Nemzek, Charles W. Smith, Ruth M. Skoug and C. Robert Clauer, The solar-wind driving of global sawtooth oscillations and periodic substorms: What determines the periodicity, Submitted to *Ann Geophys.,* 2006.

Chapman, S., Earth storms: Retrospect and prospect, *J. Phys. Soc. Japan*, *17*(Suppl. A-1), 6 – 16, 1962.

Clauer, C., M. W. Liemohn, J. U. Kozyra, and M. L. Reno, The relationship of storms and substorms determined from mid-latitude ground-based magnetic maps, in *Disturbances in Geospace: The Storm - Substorm Relationship*, edited by Y. K. A. S. Sharma, and G. Lakhina, pp. 143 – 157, AGU, Washington, D.C., 2003.

Clauer, C. R., and R. L. McPherron, The relative importance of the interplanetary electrric field and magnetospheric substorms on partial ring current development, *J. Geophys. Res.*, *85*, 6747, 1980.

DeJong, Anna D. and C. Robert Clauer, Polar UVI images to study steady magnetospheric convection events: Initial results, *Geophys. Res. Lett. 32,*L24101, doi:10.1029/2005GL024498, 2005.

Dungey, J. W., Interplanetary magnetic field and the auroral zones, *Phys. Rev. Lett.*, *6*, 47, 1961.

Erickson, G. M., A quasi-static magnetospheric convection model in two dimensions, *J. Geophys. Res.*, *97*, 6505, 1992.

Fairfield, D. H., Advances in magnetospheric storm and substorm research: 1989-1991, *J. Geophys. Res.*, *97*, 10865, 1992.

Henderson M. G., G. D. Reeves, R. Skoug, M. T. Thomsen, M. H. Denton, S. B. Mende, T. J. Immel, P. C. Brandt, H. J. Singer, Magnetospheric and auroral activity during the 18 April 2002 sawtooth event, J. Geophys. Res., 111, A01S90, doi:10.1029/2005JA011111, 2006

Kamide, Y., Is substorm occurrence a necessary condition for a magnetic storm?, *J. Geomagn. Geoelectr.*, *44*, 109, 1992.

Kamide, Y., P. D. Perrault, S.-I. Akasofu, and J. D.Winningham, Dependence of substorm occurrence probability on the interplanetary magnetic field and on the size of the auroral oval, *J. Geophys. Res.*, *82*, 5,521, 1977.

Klimas, A. J., D. N. Baker, D. A. Roberts, and D. H. Fair-field, A nonlinear dynamical analogue model of geomagnetic activity, *J. Geophys. Res.*, *97*, 12253, 1992.

Liemohn, M. W., Yet another caveat to using the Desssler-Parker-Sckopke relation, *J. Geophys. Res.*, *108*(A6), doi:10.1029/2003JA009839, 2003.

Liemohn, M.W., J. U. Kozyra, V. K. Jordanova, G. V. Khazanov, M. F. Thomsen, and T. E. Cayton, Analysis of early phase ring current recovery mechanisms during geomagnetic storms, *Geophys. Res. Lett.*, *26*, 2845 – 2848, 1999. ‘

Liemohn, M. W., J. U. Kozyra, C. R. Clauer, and A. J. Ridley, Computational analysis of the near-earth magnetospheric current system during two-phase decay storms, *J. Geophys. Res.*, *106*, 29531 – 29542, 2001a.

Liemohn, M. W., J. U. Kozyra, M. F. Thomsen, , J. L. Roeder, G. Lu, J. E. Borovsky, and T. E. Cayton, Dominant role of the asymmetric ring current in producing the stormtime *Dst*, *J. Geophys. Res.*, *106*, 29531 – 29542, 2001b.

McPherron, R. L., The role of substorms in the generation of magnetic storms, in *Magnetic Storms*, edited by B. T. Tsurutani,W. D. Gonzales, Y. Kamide, and J. K. Arballo, pp. 131–147, AGU, 1997.

Pytte, T., R. L. McPherron, E. W. Hones, Jr., and H. I.West, Jr., Multiple-satellite studies of magnetospheric substorms: Distinction between polar magnetic substorms and convection-driven negative bays, *J. Geophys. Res.*, *83*, 663, 1978.

Sergeev, V., On the state of the magnetosphereduring prolonged periods of the southward oriented imf, *Phys. Solariterr. Potsdam*, *5*, 39, 1977.

Sergeev, V., R. J. Pellinen, and T. I. Pulkinnen, Steady magnetospheric convection: A review of recent results, *Space Sci. Rev.*, *75*, 551–604, 1996.

Sharma, A. S., et al., The storm-substorm relationship: Current understanding and outlook, in *Disturbances in Geospace: The Storm - Substorm Relationship*, edited by Y. K. A. S. Sharma, and G. Lakhina, pp. 1 – 14, AGU, Washington, D.C., 2003.